PHYSICAL REVIEW A VOLUME 26, NUMBER 5 NOVEMBER 1982

Optical second-harmonic generation in gases with a low-power laser

D. P. Shelton* and A. D. Buckingham
Department of Theoretical Chemistry, University Chemical Laboratory, Lensfield Road, Cambridge, United Kingdom CB2 1EW
(Received 19 October 1981)

Periodic phase matching is used to enhance the dc electric-field-induced second-harmonic generation by gases illuminated with a low-power laser beam. The theory of periodic phase matching is discussed and experiments for measuring molecular hyperpolarizabilities are described.

I. INTRODUCTION

Generation of optical second-harmonic radiation through electric dipole transitions is restricted to systems lacking a center of inversion. Application of a dc electric field reduces the symmetry of the system and makes possible dc electric-field-induced second-harmonic generation (ESHG) in an initially isotropic medium. This process has been observed in gases,[1-5] liquids,[6,7] and solids.[8] The magnitude of the second-harmonic signal has hitherto been limited by the lack of a method for achieving phase matching and therefore a high-power pulsed laser has been required in order to generate a detectable number of second-harmonic photons. We describe a means of achieving periodic phase matching; by this technique the number of second-harmonic photons is increased by a factor of $\sim 10^4$, allowing measurements to be made with a gas sample excited by a laser beam with a continuous power of about 1 W.

The phase-matching problem[9-12] arises because of the dispersion of the refractive index. The second-harmonic wave generated through the nonlinear response of the medium does not travel at the same velocity as the fundamental wave which induces it. As the length of the nonlinear medium interacting with the fundamental wave is increased, the second-harmonic waves generated at the beginning and end of the sample get progressively farther out of phase with each other and eventually they interfere destructively rather than constructively. Increasing the sample length beyond this point reduces the amplitude of the resultant second-harmonic wave. The anisotropy and birefringence of a crystal allow one to choose a direction through the crystal along which the fundamental and second-harmonic beams travel with equal velocity, thereby removing the limitation on the usable length of the nonlinear medium. Except when the second-harmonic frequency lies in a region of anomalous dispersion,[13] no comparable method exists for achieving velocity matching in an isotropic medium such as a gas.

While velocity matching in an isotropic medium cannot in general be arranged, ESHG admits the possibility of periodic phase matching. The second-harmonic wave amplitude $E^{(2\omega)}$ is proportional to the applied static field $E^{(0)}$ and the square of the optical field $E^{(\omega)}$. If the magnitude of the wave-vector mismatch of the waves $\vec{E}^{(2\omega)}$ and $\vec{E}^{(\omega)}$ in the sample is $\Delta k = (2k_\omega - k_{2\omega})$, then the second-harmonic waves generated by regions of the sample separated by the coherence length $l_c = \pi/|\Delta k|$ will be out of phase by π radians. Reversing the static field $E^{(0)}$ changes the sign of $E^{(2\omega)}$ which is equivalent to an additional phase shift of π radians. If the static field reverses with a spatial period l_c, then the phase shift of $\vec{E}^{(2\omega)}$ due to reversal cancels its phase shift due to velocity mismatch and the resultant second-harmonic waves from each segment of the sample will be in phase and interfere constructively. By matching the spatial periodicity of the electrostatic field to the coherence length l_c of the sample, the limitation on sample length due to dispersion is removed.

II. THEORY

The analysis of the problem of ESHG with a focused laser beam and a periodic electric field follows that of Ward and New.[14] We assume a static electric field

$$E_y^{(0)}(z) = E_0^{(0)} \cos(Kz)$$

and a focused Gaussian beam polarized parallel to the static electric field and propagating in the z

direction. The focusing of the beam is specified by the confocal parameter z_0, where

$$z_0=\pi r_0^2\frac{n_\omega}{\lambda_\omega} . \tag{1}$$

The beam radius is given by

$$(r/r_0)^2=1+(z/z_0)^2 , \tag{2}$$

where r_0 is the beam radius at the focus, n_ω is the refractive index, and λ_ω is the vacuum wavelength for light of frequency ω.[9] Our confocal parameter z_0 corresponds to $b/2$ of Ward and New.[14]

If the region of the sample subjected to the electrostatic field has length $2L$ and the single Gaussian-mode laser beam is focused at the center of this region, then the power $P^{(2\omega)}$ of the generated second-harmonic beam is given by

$$P^{(2\omega)}=\frac{\omega^3}{z_0\pi c n_{2\omega}^2}\left[\frac{\mu_0}{\epsilon_0}\right]^{3/2}\chi_{\rm NL}^2 P^{(\omega)2}E_0^{(0)2}\left[\int_{-L}^{L}dz\frac{\cos Kz\cos[\Delta kz-\arctan(z/z_0)]}{[1+(z/z_0)^2]^{1/2}}\right]^2 , \tag{3}$$

where $\chi_{\rm NL}$ is the nonlinear susceptibility of the sample and Δk is the wave-vector mismatch. Including local-field corrections, the nonlinear susceptibility of a gas sample is given by[15]

$$\chi_{\rm NL}=\frac{1}{4}\left[\frac{n_\omega^2+2}{3}\right]^2\left[\frac{n_{2\omega}^2+2}{3}\right]\left[\frac{\mu^{(0)}\beta}{3k_BT}+\gamma\right]\rho , \tag{4}$$

where β and γ are the appropriate components of the first and second hyperpolarizability tensors, $\mu^{(0)}$ is the permanent dipole moment, and ρ is the number density of molecules. The wave-vector mismatch Δk is determined by the difference in refractive index of the sample between frequencies ω and 2ω:

$$\Delta k=2k_\omega-k_{2\omega}=\frac{4\pi}{\lambda_\omega}(n_\omega-n_{2\omega})=\frac{-2\pi}{\lambda_\omega\epsilon_0}(\alpha_{2\omega}-\alpha_\omega)\rho+(\text{terms in }\rho^2) . \tag{5}$$

The electrode geometry of interest to us is that in which the number of periods $N=KL/\pi$ of the electrostatic field $E^{(0)}(z)$ is large. In this case the integral in Eq. (3) is sharply peaked near $|\Delta k|=K$. The peak has width proportional to $1/N$ and height proportional to N^2. Evaluating the integral, we obtain the following result for the value of the second-harmonic power when the phase mismatch has been optimized for maximum power:

$$P_{\rm opt}^{(2\omega)}=\frac{\omega^3}{\pi c n_{2\omega}^2}\left[\frac{\mu_0}{\epsilon_0}\right]^{3/2}\chi_{\rm NL}^2 P^{(\omega)2}E_0^{(0)2}L[(z_0/L)\arctan^2(L/z_0)C(L/z_0)] , \tag{6}$$

where C is a slowly varying numerical factor with a value near unity. The number of periods N enters Eq. (6) implicitly through the density ρ in $\chi_{\rm NL}$—to see this combine Eq. (4) and (5) and recall that $N\approx|\Delta k|L/\pi$—and more weakly through the dependence of $\Delta k_{\rm opt}$ and C upon N. As N increases, the value of $|\Delta k/K|_{\rm opt}$ tends to one. The values of $|\Delta k/K|_{\rm opt}$ and C also depend upon the focusing parameter L/z_0; in the weak-focusing limit both $|\Delta k/K|_{\rm opt}$ and C tend to one. Optimum focusing occurs near $L/z_0=3$. In Table I we illustrate the dependence of $|\Delta k/K|_{\rm opt}$, C, and the power $P^{(2\omega)}$ on the focusing parameter L/z_0, for $N=79$. For near-optimum focusing, the variation of the second-harmonic power is quadratic in $\chi_{\rm NL}$, $P^{(\omega)}$, and $E_0^{(0)}$, but only linear in length L.

Periodic phase matching in gases is achieved most simply by varying the density of the gas. Since the wave-vector mismatch Δk is proportional to the density ρ it is possible, for a given value of the electrostatic-field periodicity $2l=2\pi/K$, to set $|\Delta k/K|$ to its optimum value merely by adjusting the gas density. The theoretical phase-matching curve scanned by varying the gas density, and some experimental measurements of it, are plotted in Fig. 1. The second-harmonic signal and the sample density have been normalized to their values at the top of the main peak of the phase-matching curve. Weaker than optimum focusing, $L/z_0=1.09$, and an electrostatic field with $N=79$ periods have been assumed. The main peak and the subsidiary peaks are seen to have fractional widths of about $1/N$; the main peak, corresponding to optimum phase matching, is much stronger than the others. The main peak is shifted down in density by a factor of 0.9965 from the value it would

TABLE I. Dependence of the phase-matching peak position and height parameters on the focusing parameter L/z_0 for $N=79$.

L/z_0	$\lvert \Delta k/K \rvert_{opt}$	C	$[(z_0/L)\arctan^2(L/z_0)C(L/z_0)]$
0.0	1.0000	1.000	0.000
0.2	0.9993	1.012	0.197
0.5	0.9983	1.073	0.461
1.0	0.9967	1.249	0.771
1.5	0.9956	1.457	0.938
2.0	0.9948	1.662	1.019
3.0	0.9935	2.026	1.054
4.0	0.9927	2.325	1.022

have if optimum phase matching occurred at $|\Delta k| = K$.

III. EXPERIMENT

A schematic diagram of the apparatus is shown in Fig. 2. The fundamental light beam is generated by an argon-ion laser. The laser beam is weakly focused and passes through the gas sample and electrode array contained within a stainless-steel pressure vessel. The weak second-harmonic beam emerges from the sample cell colinearly with the fundamental beam and is separated from it by a combination of a double-prism monochromator and a 1-cm thick aqueous $NiSO_4$-$CoSO_4$-solution filter. The second-harmonic beam is detected by a photomultiplier tube operating in the photon-counting mode. The background count rate is separated from the second-harmonic signal by modulating the voltage applied to the electrode array and subtracting the background (high voltage off) from the signal plus background (high voltage on) in a synchronous photon counter.

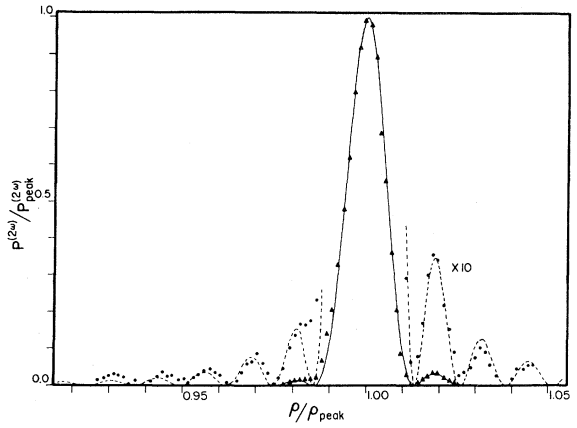

FIG. 1. Curves illustrate the calculated variation of the second-harmonic power $P^{(2\omega)}$ as the wave-vector mismatch of the sample is changed by varying the gas density ρ. The parameters assumed are $L/z_0=1.09$ and $N=79$. The points are experimental measurements. The scale has been expanded 10× for the dashed curved and the corresponding data points.

A cross section of part of the electrode array is shown in Fig. 3. The electrodes consist of steel wires 0.56 mm in diameter spaced $l=1.27$ mm apart. They are soldered into grooves milled into stainless-steel bars, so that the average spacing of the electrodes along the array is fixed and known to about 0.01%. The overall length of the array is about 20 cm and there are $2N=158$ electrode pairs. The confocal parameter of the focused laser beam is $z_0=9.2$ cm.

The optimum geometry of the electrode array has the transverse spacing of the electrodes equal to their longitudinal spacing as a compromise between two conflicting requirements. On the one hand, if the transverse spacing is made much larger than the longitudinal spacing, then the spatially periodic component of the electrostatic field on the axis of the array becomes vanishingly small compared to the field near the electrode surface. The magnitude of the field, at the electrode surface where it is greatest, may not exceed the breakdown field of the gas sample. To maximize the periodic electric field on the axis of the array, the transverse spacing of the electrodes should be made small compared to their longitudinal spacing. On the other hand, the second-harmonic power increases as the square of the number of periods N of the electrostatic field, and for a given array length N is maximized by making the longitudinal spacing as small as possible. To obtain a strong

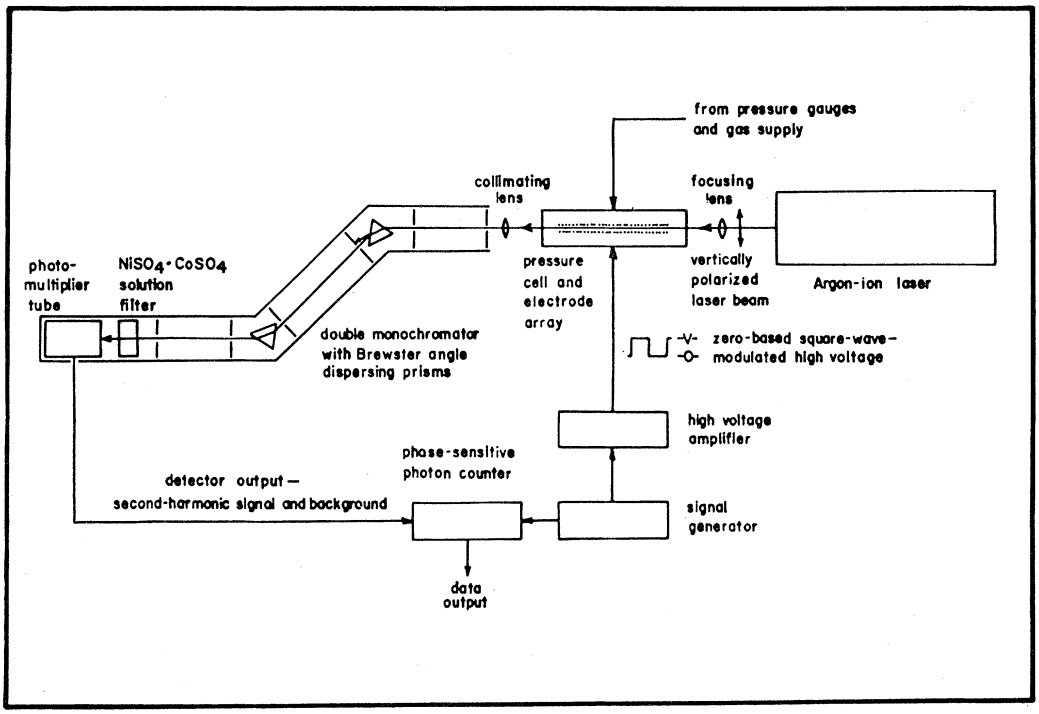

FIG. 2. Schematic diagram of the experimental apparatus, showing the cell in which the modulated ESHG beam is produced, the monochromator which separates the second-harmonic beam and the configuration of the electronics which allows phase-sensitive detection of the signal from the photomultiplier tube.

periodic field with the shortest periodicity, we have set the transverse spacing equal to the longitudinal electrode spacing.

Since the beam must pass between the electrodes without obstruction, it turns out that diffraction puts an upper bound on the attainable second-harmonic generation efficiency. Assuming the focusing parameter $L/z_0 = 1.4$, and that the trans-

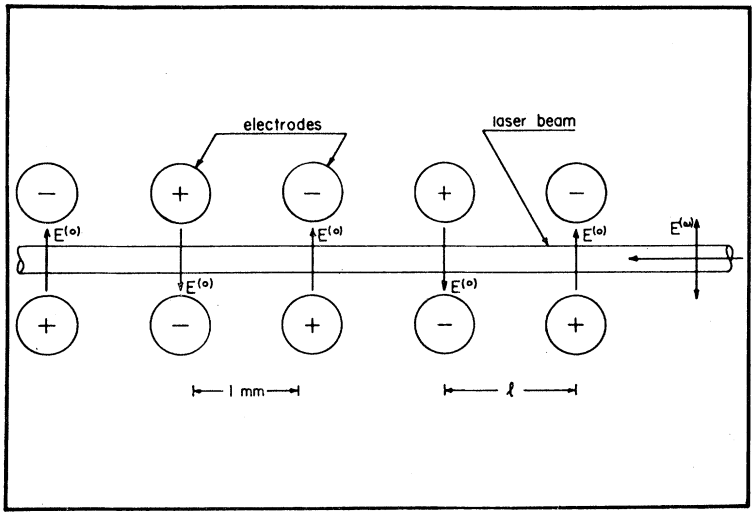

FIG. 3. Cross section of part of the electrode array, indicating the laser beam and the spatially alternating electrostatic field $E^{(0)}$ through which it passes. The array is composed of 158 pairs of wires 0.56 mm in diameter and spaced $l = 1.27$ mm apart.

verse and longitudinal electrode spacings are equal and the electrode diameter is half the spacing between the centers, the condition for the laser beam to be unobstructed is $l \approx 12 r_0$. Setting $K = \pi/l = |\Delta k|$ and using Eqs. (4), (5), and (6), we obtain the following result for ESHG by a monatomic gas in an electrode array of optimum geometry:

$$P^{(2\omega)} = 9\times 10^{-4}(\mu_0/c)P^{(\omega)2} \times E_0^{(0)2}\left[\frac{\omega\gamma}{\alpha_{2\omega}-\alpha_\omega}\right]^2 . \quad (7)$$

The frequency dependences of the polarizabilities appearing in Eq. (7) are given in the low-frequency limit of the single-resonance approximation[16] by

$$\alpha_\omega = \alpha_0[1+(\omega/\omega_1)^2] , \quad (8)$$

$$\gamma_\omega = \gamma_0[1+10(\omega/\omega_1)^2] , \quad (9)$$

$$\Delta k = \frac{-\omega}{\epsilon_0 c}(\alpha_{2\omega}-\alpha_\omega)\rho = \frac{-3\alpha_0\rho}{\epsilon_0 c\omega_1^2}\omega^3 , \quad (10)$$

where α_0 and γ_0 are the static values and ω_1 is the resonance frequency. In deriving Eq. (9) we have assumed there is actually a group of transitions near the effective resonant frequency ω_1 but that all resonance denominators are equal. Substituting these expressions into Eq. (7) yields the following expression for the frequency dependence of the maximum conversion efficiency:

$$\eta = P^{(2\omega)}/P^{(\omega)} = 4\times 10^{-19}P^{(\omega)} \times E_0^{(0)2}\left[\frac{\omega_1\gamma_0}{\alpha_0}\right]^2 \frac{1+20(\omega/\omega_1)^2}{(\omega/\omega_1)^2} . \quad (11)$$

The maximum attainable conversion efficiency decreases rapidly with increasing ω for $\omega < 0.2\omega_1$, but is almost constant for larger ω. Since the quantity $(\omega_1\gamma_0/\alpha_0)$ appearing in Eq. (11) is roughly constant for a wide range of atoms and molecules, the second-harmonic conversion efficiency η should not be strongly dependent on the particular gas comprising the sample. However, the value of η obtained with dipolar molecules may be an order of magnitude larger than that obtained with nondipolar molecules because the β term of Eq. (4) can dominate the γ term when it is not forced to vanish by symmetry.

The ESHG experiment performed with He gas as the sample in our apparatus serves to illustrate the usual operating conditions. The atomic parameters for He (Ref. 15) are

$$\omega_1 = 3.9\times 10^{16}\ \text{rad s}^{-1} ,$$

$$\alpha_0 = 2.3\times 10^{-41}\ \text{C}^2\text{m}^2\text{J}^{-1} ,$$

and

$$\gamma_0 = 2.8\times 10^{-63}\ \text{C}^4\text{m}^4\text{J}^{-3} .$$

Typical experimental parameters are

$$P^{(\omega)} = 1.5\ \text{W} ,$$

$$E_0^{(0)} = 3.0\times 10^6\ \text{V m}^{-1} ,$$

and

$$\lambda_\omega = 514.5\ \text{nm} ,$$

in which case the conversion efficiency computed from Eq. (11) is $\eta = 1.6\times 10^{-14}$. The observed conversion efficiency for He gas is close to this value. In the experiment there are 6×10^4 second-harmonic photons generated per second, of which 1×10^3 are eventually detected and counted. The background count rate is less than 100 Hz. For the interelectrode spacing used in our apparatus, periodic phase matching occurs in He at about 100 atm while in most other gases it occurs at only a few atm.

In order to determine γ directly, one must measure $P^{(\omega)}$, $E^{(0)}$, z_0, L, λ, n, ρ, and the detective quantum efficiency of the apparatus. Then the value of γ is given in terms of these quantities by Eq. (4) and (6). However, Eq. (6) must be modified by two further numerical factors. The factor $(2m-1)/m \approx 2$ accounts for the enhancement of SHG because the laser oscillates at $m \approx 30$ independent longitudinal modes.[17] The other factor arises because the electrostatic field applied to the sample is not purely sinusoidal. Numerical calculation for our electrode geometry gives

$$E^{(0)}(z) = E_0^{(0)}(1.14\cos Kz - 0.14\cos 3Kz) , \quad (12)$$

where $E_0^{(0)}$ is the peak field strength on the axis of the array. The square of the coefficient of $\cos Kz$, which is no longer just $E_0^{(0)}$, appears in the expression for $P^{(2\omega)}$. The higher spatial-frequency components of $E^{(0)}(z)$ allow periodic phase matching at multiples of the lowest phase-matching density but yield less second-harmonic power. Our experimentally determined value of γ_{He} at 514.5 nm is $2.7\pm 0.5\times 10^{-63}\ \text{C}^4\text{m}^4\text{J}^{-3}$ in agreement with the

computed value of $2.95\pm0.03\times10^{-63}$ $C^4m^4J^{-3}$.[18] Direct measurement of γ with an accuracy of a few percent seems to be possible, though difficult, by a refinement of this method. However, measurements of the ratio of γ for two different molecules are much more accurately and easily obtained. Provided a means of calibration exists (ie., the *ab initio* value of γ_{He}), this is the preferred method for measurement of hyperpolarizabilities. We discuss this method in the next section.

IV. MEASUREMENT OF HYPERPOLARIZABILITIES

The measurement of ratios of hyperpolarizabilities for different molecules depends on keeping almost all experimental parameters constant while the samples are interchanged. If the sample density is in each case adjusted to the peak of the phase-matching curve while laser power, applied electric field, and focusing are left unchanged, then from Eqs. (4) and (6) we obtain, for the ratio of the hyperpolarizabilities of molecules A and B,

$$R=\left[\gamma+\frac{\mu^{(0)}\beta}{3k_BT}\right]_A\Bigg/\left[\gamma+\frac{\mu^{(0)}\beta}{3k_BT}\right]_B$$

$$=(S_A^{(2\omega)}/S_B^{(2\omega)})\frac{n_B\rho_B}{n_A\rho_A}\,, \tag{13}$$

where $S^{(2\omega)}$ is the measured count rate of second-harmonic photons and n and ρ are the sample refractive index and density, respectively, all at optimum phase matching.

A reliable *ab initio* value is available for γ_{He} at optical frequencies[18] so that if atom B in Eq. (13) is taken to be He, then the hyperpolarizability of molecule A is simply given by the product of the experimentally measured ratio R and the *ab initio* value of γ_{He}. For dipolar molecules, the γ and β terms in Eq. (4) may both be determined by making measurements over a range of temperature; for nondipolar or centrosymmetric molecules, the term $(\mu_0^{(0)}\beta/3kT)$ vanishes, leaving only the temperature-independent γ term.

Measurements made by this method for a number of small molecules are presented in Table II. The measured values of γ and β and the sample densities ρ_{opt} at which optimum phase matching occurred are given. For the dipolar molecules, γ and β were determined from measurements over the temperature range 20—170 °C; for the other molecules the measurements were made near 20 °C. The quantity ρ_{3K} is the optimum phase-matching density when the cos3Kz component of the periodic electrostatic field or Eq. (12) produces ESHG signal.

The uncertainties quoted in Table II require some explanation. The uncertainties given for γ and β include all sources except the uncertainty of the *ab initio* value of γ_{He} used for calibration, which is thought to be about 1%.[18–20] The uncertainty of the experimentally determined ratios is in most cases smaller than 1%, so the principal limitation to the accuracy of the hyperpolarizability determination is due to the uncertainty of the calibration rather than of the ratio measurement. A better *ab initio* calculation if γ_{He} is feasible; if γ_{He} is recalculated, the uncertainty in the calibration might be eliminated and the correct values of the hyperpolarizabilities could be recovered from the values in Table II by multiplying by the ratio of the new and old values of γ_{He}. Accordingly, we have quoted the exact value of γ_{He} used for calibration and uncertainties which represent the accuracy inherent in the ratio measurement, in order that any trends present in the data are not obscured by excessive error bars.

The ratio measurements are very precise because the phase-matching peak is very narrow and because only the phase-matching density and the square root of the second-harmonic signal need to be measured. The fractional width of the phase-matching peak is only 10^{-2}; given a noise amplitude of 1% in the peak count rate $S^{(2\omega)}$ due to counting statistics and instrumental drifts, the peak of the phase-matching curve may be located with an uncertainty of less than 0.1% in density. The density of the sample is determined from its measured pressure and temperature by means of the virial equation of state including second and third virial coefficients.[21] Temperatures were measured with a platinum resistance thermometer; care was taken to ensure that thermal drifts and heating by stray laser radiation did not lead to sample inhomogeneity. The gas pressure was measured with either a Budenberg dead-weight tester at high pressures or a steel-tube mercury manometer[22] at low pressures. The accuracy of the phase-matching density determination was limited by the accuracy of the virial corrections, the gauge calibration, the sample purity, and the reproducibility of the peak-position determination, usually in that order. The precision of the measurements of $S^{(2\omega)}$ was limited by counting statistics and drifts in laser power. Refractive indices were derived from the litera-

TABLE II. Hyperpolarizabilities and phase-matching densities of several molecules, measured at 514.5 nm.

Molecule	$10^{63}\gamma$ ($C^4\,m^4\,J^{-3}$)[a]	$10^{53}\beta$($C^3\,m^3\,J^{-2}$)[a]	ρ_{opt} (mole m^{-3})[b]	ρ_{3K} (mole m^{-3})[c]	$10^{59}\gamma\rho_{opt}$ ($C^4\,m\,J^{-3}$ mole)
He	2.950[d]		4690±3		1.4
Ar	95.4±0.2		236.8±0.2		2.3
H_2	57.1±0.1		322.7±0.2		1.8
N_2	73.4±0.3		220.7±0.2		1.6
CO_2	99.0±0.5		125.32±0.02		1.2
CH_4	248.2±0.4		98.97±0.02	297.9±0.2	2.5
CH_3F	161±16	−184±4	121.6±0.2	367±1	2.0
CHF_3	109±5	−88±2	174.9±0.4		1.9
CF_4	76.9±0.8		220.8±0.2		1.7
SF_6	107±1		127.7±0.4		1.4

[a]Error estimates exclude the uncertainty of γ_{He} used for calibration.
[b]Measured at $|\Delta k|_{opt}=2465.0\pm0.5\ m^{-1}$.
[c]Measured at $|\Delta k_{3K}|_{opt}=7412.4\pm1.5\ m^{-1}$.
[d]Calculated value from Ref. 18; assumed in calibrating the other measurements.

ture[23]; they contribute only a very small correction in determining the hyperpolarizabilities. The sign of the hyperpolarizability was determined using mixed-gas samples.[3]

Accurate measurements were possible with laser power in the range from 0.2 W up to the maximum available power of 2.5 W. Thus, we were able to measure γ_{CH_4} at six of the argon-ion laser frequencies. The results are presented in Table III and Figs. 4 and 5. The uncertainty in the values of $\gamma_{He}(\omega)$ used for calibration are not expected to affect significantly the shape of the dispersion curve for $\gamma_{CH_4}(\omega)$.

The optimum phase-matching density ρ is obtained as a by-product of the hyperpolarizability measurement. Since $\Delta k_{opt}\approx K$ is fixed by the interelectrode spacing, the value of $(\alpha_{2\omega}-\alpha_\omega)$ is just proportional to ρ_{opt}^{-1}. The approximate constancy of

$$(\omega_1\gamma_0/\alpha_0)\approx\omega\gamma/(\alpha_{2\omega}-\alpha_\omega)$$

mentioned in connection with Eq. (11) is illustrated in Table II, where the product $\gamma\rho_{opt}$ is seen to be more nearly constant than γ or ρ_{opt} separately.

V. DISCUSSION

In the low-frequency limit of the single-resonance approximation, Eqs. (9) and (10), we find that $\gamma(\omega)$ is linear in ω^2, while $\rho_{opt}^{-1}\propto(\alpha_{2\omega}-\alpha_\omega)$

TABLE III. Frequency dependence of the hyperpolarizability and phase-matching density for He and CH_4.

λ (nm)	$10^{63}\gamma_{He}$ ($C^4\,m^4\,J^{-3}$)[a]	ρ_{He} (mole m^{-3})[b]	$10^{63}\gamma_{CH_4}$ ($C^4\,m^4\,J^{-3}$)[c]	ρ_{CH_4} (mole m^{-3})[b]
694.3	2.820	11 620±12[d]	196±2[e]	270±3[e]
514.5	2.950	4 690±3	248.2±0.4	98.97±0.02
501.7	2.965	4 346±2	250.8±1.1	90.71±0.08
496.5	2.972	4 205±2	259.2±2.0	87.51±0.02
488.0	2.983	3 987±2	267.4±1.6	82.26±0.04
476.5	3.000	3 698±2	269.7±1.0	75.75±0.07
457.9	3.030	3 265±2	279.5±0.9	65.58±0.07

[a]Calculated values from Ref. 18; assumed in calibrating the γ_{CH_4} measurements.
[b]Measured at $|\Delta k|_{opt}=2465.0\pm0.5\ m^{-1}$.
[c]Error estimates exclude the uncertainty of γ_{He} used for calibration.
[d]From Ref. 1.
[e]From Ref. 4.

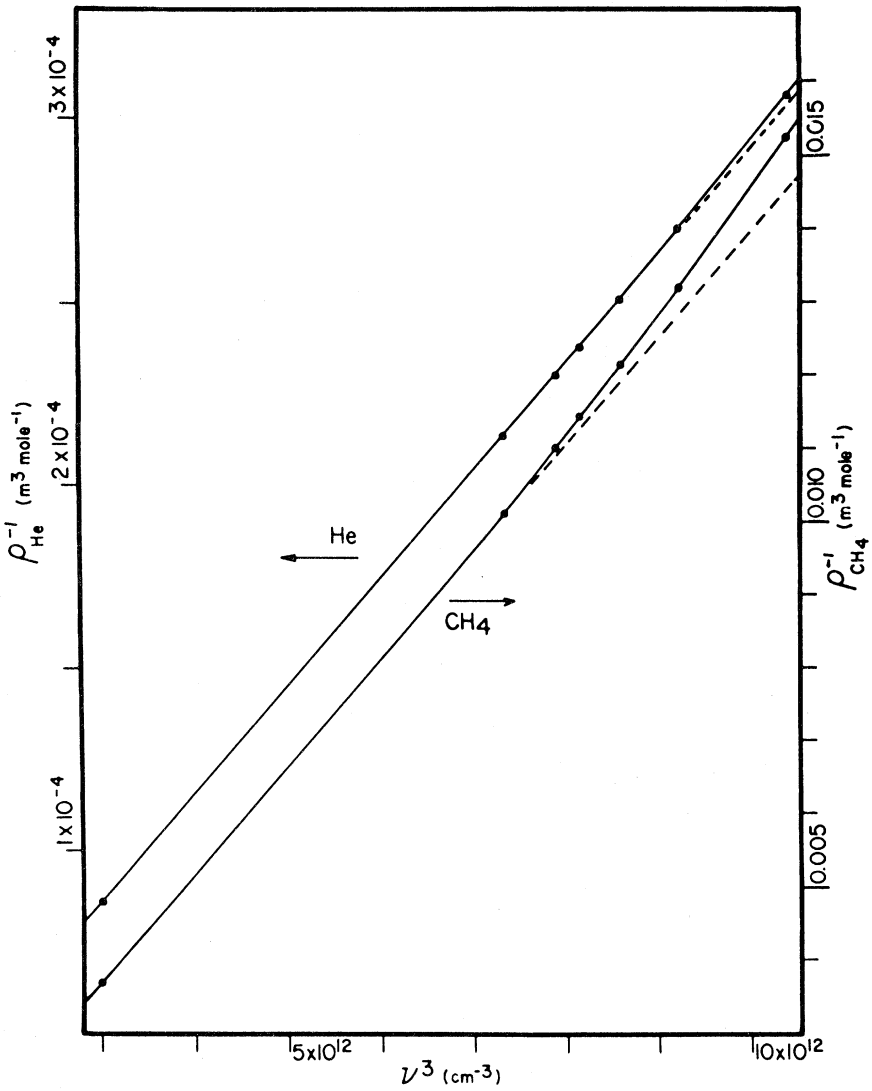

FIG. 4. Experimental measurements for He and CH_4 of the inverse phase-matching density ρ^{-1} are plotted vs the cube of the incident-light frequency ν. Straight lines fitting the data at low frequency are shown by the dashed lines.

varies as ω^3. Thus, we have plotted ρ_{opt}^{-1} vs ω^3 and $\gamma(\omega)$ vs ω^2 in Figs. 4 and 5, respectively, for He and CH_4. The straight-line fit predicted by the single-resonance model seems to be a good first approximation to the data. The measured values of ρ_{opt}^{-1} in Fig. 4 deviate from a straight line at high frequencies; for CH_4 the fractional deviation at the highest frequency is 0.05. The expected correction to our approximation for this case is of order $(\omega/\omega_1)^2 = 0.05$.[24] For He, the deviation of the measurements from the straight line is four times smaller than for CH_4, in accord with the resonance frequency ω_1 for He being twice as large as for CH_4. So it seems that the variation of $(\alpha_{2\omega} - \alpha_\omega)$ with frequency can be understood in terms of the simple, single-resonance model. In Fig. 5, we see that the straight-line fit to the *ab initio* values of γ_{He} agrees very well. The measured values of γ_{CH_4} also lie near a straight line, but the observed deviations do not seem explicable in terms of the single-resonance model. When the differences between the measured values of γ_{CH_4} and the straight line passing through the points in Fig. 5 are plotted, one gets the "resonance" shape shown in the inset.

The only excitations of the CH_4 molecule which have energies near that of the resonance in the $\gamma_{CH_4}(\omega)$ plot are the highly excited vibrations. For

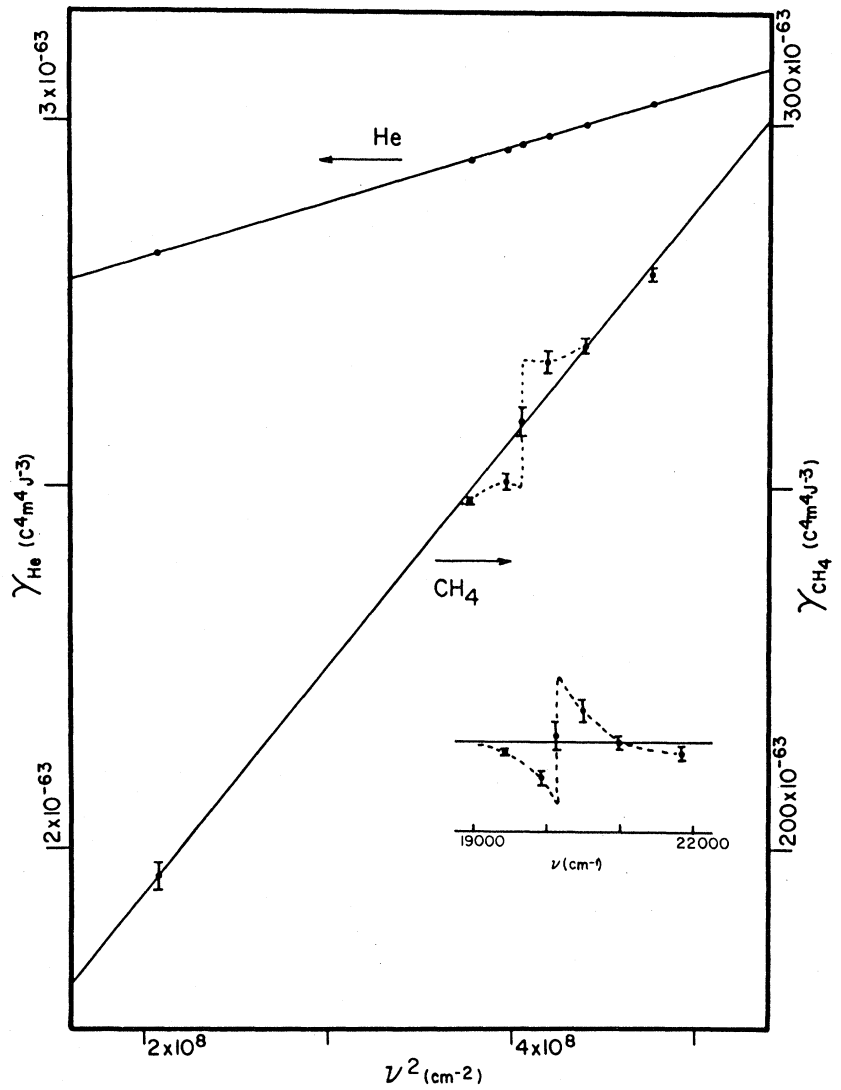

FIG. 5. Calculated values of γ for He and the experimentally measured values of γ for CH_4 are plotted vs the square of the incident-light frequency ν. Straight lines fitting through the points are shown solid. For CH_4, the difference between the straight line and the data points is plotted vs frequency in the inset. The resonance in γ_{CH_4} at $\nu=20\,140$ cm^{-1} is indicated by the dashed curves.

high vibrational excitations, a local-mode description[25–27] is appropriate and there is only a single set of CH-stretching vibrational frequencies. For CH_4, these transition frequencies are given by

$$\omega(0\rightarrow v)=v\omega_i+v^2x_{ii}\ , \tag{14}$$

where $\omega_i=3077$ cm^{-1} and $x_{ii}=-64$ cm^{-1}.[28] The width of the absorption bands due to these transitions is typically 300 cm^{-1} for $v=5$ and decreases with increasing v. The $\Delta v=8$ vibrational transition expected at 20 520 cm^{-1} falls close to the position of the observed resonance in γ_{CH_4} which lies at 20 140 cm^{-1} and has a width of about 200 cm^{-1}. If the feature observed in the γ_{CH_4} vs ω plot is due to a vibrational transition, then Eq. (14) predicts several more resonances. However, the frequencies at which we made measurements in the present experiment did not coincide with any of the other predicted resonance frequencies.

While the match between the frequency of the observed resonance and of the $\Delta v=8$ vibrational transition in CH_4 is satisfactory, the amplitude of the resonance is not in such good agreement with theoretical estimates. The pertubration theoretic expression for the second hyperpolarizability measured in our experiment is[29]:

$$Y_{zzzz}(-\omega_\sigma;\omega_1,\omega_2,\omega_3)=6\frac{e^4}{\hbar^3}I_{-\sigma,1,2,3}\left[\sum_{lmn}{}'\frac{\langle g\,|\,z\,|\,l\rangle\langle l\,|\,z\,|\,m\rangle\langle m\,|\,z\,|\,n\rangle\langle n\,|\,z\,|\,g\rangle}{(\omega_{lg}-\omega_\sigma)(\omega_{mg}-\omega_1-\omega_2)(\omega_{ng}-\omega_1)}\right.$$

$$\left.-\sum_{lm}{}'\frac{\langle g\,|\,z\,|\,l\rangle\langle l\,|\,z\,|\,g\rangle\langle g\,|\,z\,|\,m\rangle\langle m\,|\,z\,|\,g\rangle}{(\omega_{lg}-\omega_\sigma)(\omega_{mg}-\omega_1)(\omega_{mg}+\omega_2)}\right], \tag{15}$$

where $I_{-\sigma,1,2,3}$ denotes the average over the expressions obtained by permuting the frequencies $-\omega_\sigma=-2\omega$, $\omega_1=0$, and $\omega_2=\omega_3=\omega$.

Far below resonance we may write an expression for γ in terms of the transition polarizabilities α_{gm},

$$\gamma^{\text{nonres}}=\tfrac{3}{2}\sum_m{}'\frac{(\alpha_{gm})^2}{\hbar\omega_{mg}}-\frac{3}{2}\frac{(\alpha_{gg})^2}{\hbar\omega_{mg}}, \tag{16}$$

where ω_{mg} is the typical electronic transition frequency and the sum includes those electronic states which may be reached by a series of strong transitions from the ground state $|g\rangle$. If for CH_4 we take

$$\alpha_{gg}=\alpha_{gm}=3\times10^{-40}\ \text{C}^2\,\text{m}^2\,\text{J}^{-1}$$

(Ref. 15),

$$\omega_{mg}=2\times10^{16}\,\text{rad}\,\text{s}^{-1}$$

(Ref. 24), and the number of upper electronic states in the sum as four, we compute the value

$$\gamma^{\text{nonres}}=+0.2\times10^{-60}\,\text{C}^4\,\text{m}^4\,J^{-3}$$

as compared to values in the range

$$0.2-0.3\times10^{-60}\ \text{C}^4\,\text{m}^4\text{J}^{-3}$$

measured at optical frequencies.

An expression for the resonant part of γ, due to a transition to the vibrationally excited ground electronic state $|v\rangle$, may be written by including damping and retaining those terms containing the resonance denominator $(\omega_{vg}-\omega-i\Gamma_{vb}/2)$ The resulting approximation for the change in γ on going through resonance (from $\omega=\omega_{vg}-\Gamma_{vg}/2$ to $\omega_{vg}+\Gamma_{vg}/2$) is given by

$$\Delta\gamma^{\text{res}}=-\tfrac{1}{2}\frac{(\alpha_{gg})^2}{\hbar\omega_{mg}}\left[\frac{\alpha_{gv}}{\alpha_{gg}}\right]^2\times\left[\frac{\omega_{mg}}{\Gamma_{vg}}\right]\left[1-\tfrac{1}{2}\frac{\omega_{mg}}{\omega_{vg}}\right]. \tag{17}$$

Evaluating Eq. (17) with $\omega_{mg}=10^5\ \text{cm}^{-1}$, $\omega_{vg}=2\times10^4\ \text{cm}^{-1}$, $\Gamma_{vg}=200\ \text{cm}^{-1}$, and $(\alpha_{gv}/\alpha_{gg})=10^{-6}$, one gets the result $(\Delta\gamma^{\text{res}}/\gamma^{\text{nonres}})=1\times10^{-10}$. The measured value of this quantity is $(\Delta\gamma^{\text{res}}/\gamma^{\text{nonres}})_{\text{exp}}=+5\times10^{-2}$. Our calculation correctly predicts the sign of $\Delta\gamma^{\text{res}}$. The resonance is inverted; at first γ decreases as the resonance frequency is approached from below, and then it rapidly increases as ω passes through resonance. The calculated magnitude of $\Delta\gamma^{\text{res}}$, however, is nearly nine orders of magnitude too small. The calculated value of $\Delta\gamma^{\text{res}}$ depends strongly on the assumed value of $(\alpha_{gv}/\alpha_{gg})$; our estimate of $(\alpha_{gv}/\alpha_{gg})$ for the $\Delta v=8$ vibrational transition of CH_4 is based on an extrapolation of the calculated values of α_{gv} for H_2 with $\Delta v\leq4$.[30–32] The size of α_{gv} depends chiefly on the anharmonicity of the vibrations and it is possible that our estimate is too low by more than an order of magnitude because we have extrapolated from small Δv. Equation (17) gives the contribution from a single vibrational transition; in the local-mode description there are nearly 2000 quasidegenerate states in which eight vibrational quanta are distributed over the four CH bonds.[25] If, in addition, the linewidth Γ_{vg} of each of these individual transitions were several times narrower than the aggregate width of the band, then our estimate of $\Delta\gamma^{\text{res}}$ could be increased by a factor of 10^4 or more because of the multiplicity of states. All this considered, it is possible that our first estimate of $\Delta\gamma^{\text{res}}$ is too low by a factor of 10^6-10^8, and our interpretation of the resonance in γ_{CH_4} as due to a vibrational transition may be sound after all.

In order to test the accuracy of the phase-matching density determination and the internal consistency of the experimental method, we have used the $\cos3Kz$ component of the electrostatic field of Eq. (12) to achieve phase matching at a density ρ_{3K}, nearly three times the density of the main phase-matching peak. Including first- and second-refractive-index virial coefficients[33,34] we get the following relation between the wave-vector mismatch Δk and the gas density ρ:

$$-\Delta k=\frac{4\pi}{\lambda_\omega}(n_{2\omega}-n_\omega)=\frac{2\pi}{\lambda_\omega\epsilon_0}\rho(\alpha_{2\omega}-\alpha_\omega)\left[1+\frac{\rho(\alpha_{2\omega}+\alpha_\omega)}{12\epsilon_0}+\frac{\rho(\alpha_{2\omega}^2+\alpha_{2\omega}\alpha_\omega+\alpha_\omega^2)}{2\pi\epsilon_0^2\sigma^3}\right.$$

$$\left.\times\int_0^\infty dx\,x^{-4}\exp(-U/k_BT)\right], \tag{18}$$

where $x=r/\sigma$ and U is the potential energy of an interacting pair of molecules. The second expression in ρ^2 is actually $6\pi\lambda_\omega^{-1}\rho^2(B_{2\omega}-B_\omega)$ where B_ω is the second-refractivity virial coefficient[33] and (18) is obtained by assuming that the change of polarizability of an interacting pair is $4\alpha^3r^{-6}\times(4\pi\epsilon_0)^{-2}$. The optimum value of the wave-vector mismatch Δk_{opt}, is determined by the interelectrode spacing, the degree of focusing, and the number of periods of the electrostatic field. For our apparatus we have

$$|\Delta k|_{\text{opt}}=0.9965(\pi/l)=2456.0\pm0.5\ \text{m}^{-1}$$

and

$$|\Delta k_{3K}|_{\text{opt}}=0.9988(3\pi/l)$$
$$=3(2470.8\pm0.5\ \text{m}^{-1})\ .$$

In Table IV we have compared the measured and calculated ratios $(\Delta k\rho_{3K}/\Delta k_{3K}\rho)_{\text{opt}}$ for CH_4 and CH_3F. The small discrepancy between the measured and calculated ratios may be due to a difference between the supposed and actual focal parameters of the laser beam or to an inadequacy of the expression for the refractive-index virial coefficients. The theory seems to be consistent with the measurements at the 0.1% level of accuracy.

VI. CONCLUSION

We have demonstrated the method of periodic phase matching, which allows one to produce a measurable ESHG signal intensity from a gas sample illuminated by a low-power laser. While the maximum second-harmonic conversion efficiency which may be attained by this method is much less that unity, periodic phase matching does permit very simple and accurate measurements of molecular hyperpolarizabilities to be made. The hyperpolarizabilities for several molecules have been reported herein, measured more accurately and at a different frequency than previously. In the course of measuring the frequency dependence of γ for CH_4 we have discovered what appears to be a resonance arising from the excitation of a high vibrational overtone of the molecule. Resonances at several other frequencies may be found for this molecule. In summary, ESHG with periodic phase matching is found to be a sensitive method for investigating the nonlinear optical response of molecules in the gas phase.

TABLE IV. Comparison of measured and calculated phase-matching density ratios.

Molecule	$\left(\frac{\Delta k}{\Delta k_{3K}}\frac{\rho_{3K}}{\rho}\right)_{\text{expt}}$	$\left(\frac{\Delta k}{\Delta k_{3K}}\frac{\rho_{3K}}{\rho}\right)_{\text{calc}}$
CH_4	$1+0.9\pm1.5\times10^{-3}$	$1-1.6\times10^{-3}$
CH_3F	$1+3.6\pm5.0\times10^{-3}$	$1-2.8\times10^{-3}$

*Present address: Department of Physics, University of Toronto, Toronto, Ontario, M5S 1A7, Canada.

[1]R. S. Finn and J. F. Ward, Phys. Rev. Lett. 26, 285 (1971).
[2]I. J. Bigio and J. F. Ward, Phys. Rev. A 9, 35 (1974).
[3]R. S. Finn and J. F. Ward, J. Chem. Phys. 60, 454 (1974).
[4]C. K. Miller and J. F. Ward, Phys. Rev. A 16, 1179 (1977).
[5]G. Hauchecorne, F. Kerhervé, and G. Mayer, J. Phys. (Paris), 32, 47 (1971).
[6]B. F. Levine and C. G. Bethea, J. Chem. Phys. 63, 2666 (1975).
[7]B. F. Levine, in *Dielectric and Related Molecular Processes,* edited by M. Davies (Chemical Society of London, London, Specialist Periodical Report, 1977), Vol. 3, p. 73.
[8]R. W. Terhune, P. D. Maker, and C. M. Savage, Phys. Rev. Lett. 8, 404 (1962).
[9]A. Yariv, *Introduction to Optical Electronics* (Holt, Rinehart, and Winston, New York, 1976).
[10]J. A. Armstrong, N. Bloembergen, J. Ducuing, and P. S. Pershan, Phys. Rev. 127, 1918 (1962).
[11]G. D. Boyd, A. Ashkin, J. M. Dziedzic, and D. A. Kleinman, Phys. Rev. 137, A1305 (1965).
[12]D. A. Kleinman, A. Ashkin, and G. D. Boyd, Phys. Rev. 145, 338 (1966).
[13]H. Puell, K. Spanner, W. Falkenstein, W. Kaiser, and C. R. Vidal, Phys. Rev. A 14, 2240 (1976).
[14]J. F. Ward and G. H. C. New, Phys. Rev. 185, 57 (1969).
[15]M. P. Bogaard and B. J. Orr, in *International Review of Science, Physical Chemistry, Ser. 2, Vol. 2, Molecular Structure and Properties,* edited by A. D. Buckingham (Butterworths, London, 1975), p. 149.
[16]E. L. Dawes, Phys. Rev. 169, 47 (1968).
[17]G. E. Francois, Phys. Rev. 143, 597 (1966).
[18]P. Sitz and R. Yaris, J. Chem. Phys. 49, 3546 (1968).
[19]A. D. Buckingham and P. G. Hibbard, Symp. Faraday Soc. 2, 41 (1968).
[20]R. Klingbeil, Phys. Rev. A 7, 48 (1973).
[21]J. H. Dymond and E. B. Smith, *The Virial Coefficients of Pure Gases and Mixtures* (Clarendon, Oxford, 1980).
[22]W. T. Lindsay and T. S. Bulischeck, Rev. Sci. Instrum. 41, 149 (1970).
[23]Landolt-Bornstein, *Zahlenwerte und Functionen, Band II,* Tiel 8 (Springer, Berlin, 1962).
[24]G. Herzberg, *Electronic Spectra of Polyatomic Molecules* (Van Nostrand-Reinhold, New York, 1966).
[25]I. A. Watson, B. R. Henry, and I. G. Ross (unpublished).
[26]B. R. Henry, Acc. Chem. Res. 10, 207 (1977).
[27]R. J. Hayward and B. R. Henry, J. Mol. Spectrosc. 57, 221 (1975).
[28]B. R. Henry (private communcation).
[29]B. J. Orr and J. F. Ward, Mol. Phys. 20, 513 (1971).
[30]J. D. Poll, in *Planetary Atmospheres,* International Astronomical Union Symp. No. 40, edited by Sagan *et al.* (Reidel, Dordrecht, 1971), p. 384.
[31]G. Karl, J. D. Poll, and L. Wolniewicz, Can. J. Phys. 53, 1781 (1975).
[32]J. Rychlewski, Mol. Phys. 41, 833 (1980).
[33]A. D. Buckingham and C. Graham, Proc. R. Soc. (London), Sect. A 337, 275 (1974).
[34]J. M. St.-Arnaud and T. K. Bose, J. Chem. Phys. 65, 4854 (1976).